

## Preliminary Numerical Analysis of Convective Heat Transfer Loop Using MARS Code

Yongjae I, Gwang Hyeok Seo, Gyoodong Jeun, Sung Joong Kim\*  
Department of Nuclear Engineering, Hanyang University  
222 Wangsimni-ro, Seongdong-gu, Seoul, 133-791, Republic of Korea  
\*Corresponding author: sungkim@hanyang.ac.kr

### 1. Introduction

The MARS code developed at Korea Atomic Energy Research Institute (KAERI) is a realistic thermal-hydraulic system analysis code with multi-dimensional analysis capability. The MARS has been developed adopting two major modules: RELAP5/MOD3 (USA) for one-dimensional (1D) two-fluid model for two-phase flows and COBRA-TF code for a three-dimensional (3D), two-fluid, and three-field model [1]. In addition to the MARS code, TRACE (USA) is a modernized thermal-hydraulics code designed to consolidate and extend the capabilities of NRC's 3 legacy safety code: TRAC-P, TRAC-B and RELAP. CATHARE (French) is also thermal-hydraulic system analysis code for Pressurized Water Reactor (PWR) safety.

There are several researches on comparing experimental data with simulation results by the MARS code. Kang et al. conducted natural convection heat transfer experiments of liquid gallium loop, and the experimental data were compared to MARS simulations [2]. Bang et al. examined the capability of the MARS code to predict condensation heat transfer experiments with a vertical tube containing a non-condensable gas [3]. Moreover, Lee et al. adopted MELCOR, which is one of the severe accident analysis codes, to evaluate several strategies for the severe accident mitigation [4].

Furthermore, recently an education program for undergraduate students has been performed at three nuclear engineering schools in Metro-Seoul: Kyung Hee University (KHU), Hanyang University (HYU), and Seoul National University (SNU). In HYU, currently experimental program using a convective heat transfer loop have been scheduled. Consequently, the objective of this study is to conduct the preliminary numerical analysis for the experimental loop at HYU using the MARS code, especially in order to provide relevant informations on upcoming experiments for the undergraduate students.

### 2. Description of MARS models

#### 2.1 Test Facility for Convective Heat Transfer Loop at Hanyang University

The forced convective heat transfer loop was developed focusing on measuring the pressure drop and heat transfer coefficient (HTC). The experiments are performed with deionized (DI) water, which is used as a coolant in the loop, under atmospheric pressure.

The test procedure is summarized in the following descriptions. The pre-heater heats up the coolant, and then the coolant moves into the test section. The heat exchanger cools down the heated coolant from the test section. As a result, the constant inlet temperature of the coolant can be obtained during the experiments. Figure 1 shows a schematic of the convective heat transfer loop.

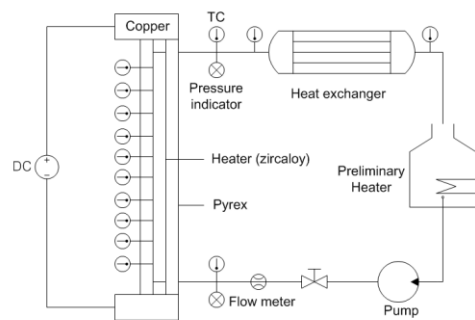


Fig. 1 Schematic of convective heat transfer loop

Figure 2 shows a schematic of the test section. The test section is composed of the heater and the Pyrex tube for a visualization work. The outside of the heater is made with a zircaloy-4 tube, and the inside of the heater is made with alumina for insulation. The heater is powered through a DC power supply, whose maximum voltage and current are 10V and 1200A, respectively. The length, diameter and thickness of the heater are 600, 7.9 and 0.8 mm, respectively. The length, diameter and thickness of the Pyrex tube are 600, 25.22 and 2.65 mm, respectively.

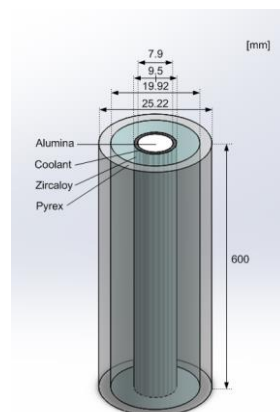


Fig. 2 Schematic of test section

Figure 3 shows a schematic of the heating element in the text section. 10 thermocouples (T/Cs) for measuring wall temperature are inserted in the holes positioned radially.

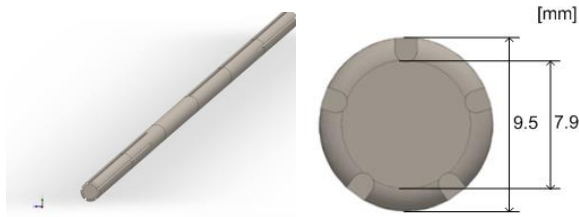


Fig. 3 Schematic of the heating element in the test section

Other T/Cs are set in the inlet and outlet of the test section. A pressure indicator is also installed in for measuring pressure drop. A flow meter is positioned between the pump and the inlet for measuring the flow rate. Table I shows summarized test sensors and their measurement ranges.

Table I: Test sensor and measurement range

| Test sensor              | Measurement range |
|--------------------------|-------------------|
| T/C (K)                  | up to 1500        |
| Pressure Indicator (bar) | 0-10              |
| Flowmeter (lpm)          | 2.8-28.4          |

## 2.2 Description of MARS Modeling

For the MARS simulation, the test section was divided into three parts: the heating part, the inlet and outlet parts. The test section was modeled as three hydrodynamic components and two heat structures. Figure 4 shows a schematic of the test section nodalization. The heating part was modeled as a pipe component with 10 volumes and 9 junctions. A time-dependent volume and a time-dependent junction were assigned to the inlet part. The outlet part was represented by a time-dependent volume and a single junction. A flow rate was defined at the time-dependent junction in the inlet part. A pressure boundary condition was applied to the outlet part. The applied mass flow rates were varied in a range of 2.85 to 28.5 lpm. The inlet temperature and pressure were 293 K and 101.325 kPa, respectively. The applied thermal power was varied in a range of 0 to 12 kW. Initial conditions are summarized in Table II.

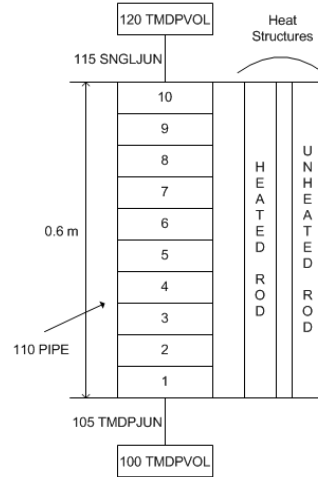


Fig. 4 MARS nodalization of the test section

Table II : Initial condition of the MARS modeling

| Variable        | Initial condition |
|-----------------|-------------------|
| Temperature (K) | 293               |
| Flow rate (lpm) | 2.85 - 28.5       |
| Power (kW)      | 0 - 12            |

## 3. Results and Discussion

For the upcoming experiments of single-phase flow for the convective heat transfer loop at Hanyang University, preliminary numerical calculations were carried out using the MARS code. As initial conditions, various flow rates and thermal power were applied to the test section.

### 3.1 Variation of Outlet and Heating Surface Temperatures

As the power was applied, the coolant left the heating part with the thermal energy transferred from the applied power. Figure 5 shows that the thermal energy transferred to the coolant with the power applied to the heating section.

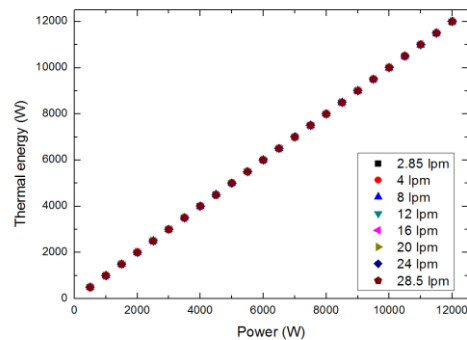


Fig. 5 Variation of thermal energy transferred to coolant with power applied to heater

Figure 6 shows a variation of the outlet temperatures with different flow rates. The coolant moves upward carrying the thermal energy generated in the heating part, and the energy heats up the coolant. As a result, the coolant temperature increases. The thermal energy taken by the coolant is calculated with Eq. (1). Moreover, as shown Fig. 6, the higher the flow rates, the lower the temperatures of the heater surface.

$$Q = c_p \dot{m}(T_{outlet} - T_{inlet}) \quad (1)$$

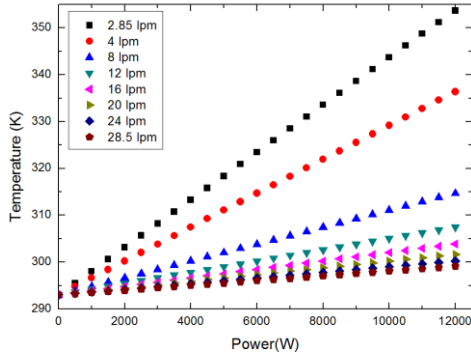


Fig. 6 Outlet temperatures of the coolant with applied flow rates

Figure 7 shows the temperatures of the heating surface with the applied power and flow rates. The surface or wall temperatures ( $T_{wall}$ ) is calculated with Eq. (2).

$$q'' = h(T_{wall} - T_{coolant}) \quad (2)$$

As shown in Fig. 7, the wall temperature increases gradually with higher applied power. In general, when the wall temperature exceeds the saturation temperature, vapor bubble could be developed, which implies that a condition of single-phase flow in the tests is not satisfied. Thus, these numerical results can give basic limitations on applied power for conducting practical experiments.

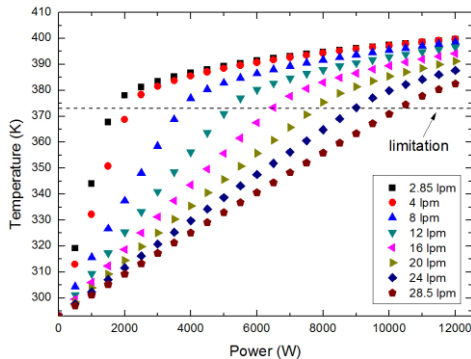


Fig. 7 Surface temperatures in the top region of the heater (axial node of heat structure: 10)

### 3.2 Variation of Pressure Drop and Heat Transfer Coefficient

In addition to the power limitations, pressure drops and HTC were calculated. Figure 8 shows the calculation results of pressure drops with the applied powers and flow rates.

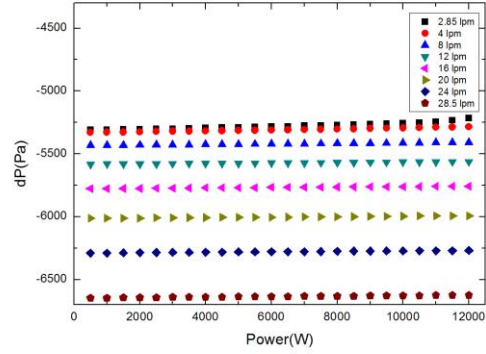


Fig. 8 Variation of pressure drop with power

The calculation results can be compared with an analytic solution using the Navier-Stokes equation with an assumption of incompressible fluid as presented in Eq. (3).

$$0 = \rho \vec{g} - \nabla \vec{P} + \mu \nabla^2 \vec{v} \quad (3)$$

Figure 9 shows a comparison of HTCs calculated by MARS and predicted by the Dittus-Boelter correlation. The Dittus-Boelter correlation, as shown in Eq. (4), is widely used for HTC or Nusselt Number. The model is valid under the conditions of  $0.7 \leq Pr \leq 160$ ,  $Re > 10^4$ , and  $L/D \geq 10$ .

$$Nu = \frac{D_e h}{k} = 0.023 Re^{0.8} Pr^{0.4} \quad (4)$$

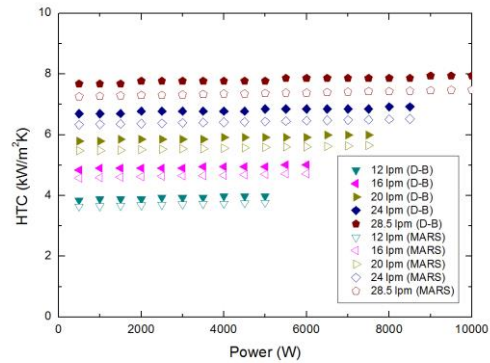


Fig. 9 Comparison of HTCs by the Dittus-Boelter correlation and MARS

## 4. Conclusion

In this study, the preliminary numerical analysis for the convective heat transfer loop was carried out using

the MARS Code. The major findings from the numerical simulations can be summarized as follows.

(1) In the calculations of the outlet and surface temperatures, the several limitations were suggested for the upcoming single-phase flow experiments.

(2) The comparison work for the HTC's shows validity for the prepared input model. This input could give useful information on the experiments.

(3) Furthermore, the undergraduate students in department of nuclear engineering, who are going to be taken part in the experiments, could prepare the program with the input, and will be provided with expected results for the single-phase and forced convective phenomena.

For the future study, different materials for the heating part are considered, such as other metals or silicon carbide (SiC) tube, which is a candidate material of fuel claddings for current and next-generation reactors.

### **Acknowledgements**

This work was supported by the National Research Foundation of Korea (NRF) grant funded by Ministry of Science, ICT and Future Planning (MSIP) with grant number, 2012M2B2A6029184.

### **REFERENCES**

- [1] Thermal Hydraulic Safety Research Department, "MARS code manual volume II: Input Requirements", Korea Atomic Energy Research Institute, 2009.
- [2] S. Kang, K. S. Ha, H. T. Kim, J. H. Kim, and I. C. Bang, An experimental study on natural convection heat transfer of liquid gallium in a rectangular loop, *International Journal of Heat and Mass Transfer*, Vol.66, pp. 192-199, 2013.
- [3] Y. S. Bang, J. H. Chun, B. D. Chung and G. C. Park, Improvements of Condensation Heat Transfer Models in MARS Code for Laminar Flow in Presence of Non-Condensable Gas, *Nuclear Engineering and Technology*, Vol. 41, No.8, pp. 1015-1024, 2009
- [4] S. N. Lee, K. S. Ha, H. Y. Kim and S. J. Kim, Validation of RCS depressurization strategy and core coolability map for independent scenarios of SBLOCA, SBO, and TLOFW, *Journal of Nuclear Science and Technology*, Vol.51 No.2, pp. 181-195, 2014
- [5] M. M. El-Wakil, *Nuclear Heat Transport*, American Nuclear Society, pp. 243-244, 1981.